OPEN FILE
855
GEOLOGICAL SURVEY
OTTAWA

GEOLOGICAL SURVEY OF CANADA

DEPARTMENT OF ENERGY MINES, AND RESOURCES

REPORT OF A GRAVITY SURVEY ACROSS THE NORMAN RANGE, NORTHWEST TERRITORIES

OPEN FILE 855

by

D.D. Lawton

This document was produced
by scanning the original publication.

Ce document est le produit d'une
numérisation par balayage
de la publication originale.

REPORT OF A GRAVITY SURVEY ACROSS THE NORMAN RANGE, NORTHWEST TERRITORIES

This report is in fulfillment of DSS Contract No. 14 SU.23294-0-0594 issued by the Department of Supply and Services, Energy, Mines and Resources, on behalf of the Institute of Sedimentary and Petroleum Geology, a division of the Geological Survey of Canada.

SUMMARY

A gravity profile 16 km in length was established across the Norman Range of the northern Franklin Mountains, Northwest Territories. A positive residual Bouguer gravity anomaly was observed over the range with a relative maximum of + 70 μms^{-2} located about 4 km southwest of the summit. The gravity anomalies were interpreted in terms of the density structure of the Norman Range and yielded two possible solutions.

(a) Saline River detachment model. In this model, the Norman Range is interpreted to be formed by a low-angle thrust involving detachment at or within the Upper Cambrian Saline River Formation. Older Proterozoic sediments are inferred not to be involved in the deformation. The model requires a minimum of 9 km of southwest to northeast horizontal shortening of the post-Proterozoic sedimentary cover.

(b) Proterozoic detachment model. In this model, the Norman Range is interpreted to be formed by a high-angle thrust involving detachment within or below the Proterozoic. The high-angle thrust results in horizontal shortening of only about 3 km.

Model (a) is preferred to model (b) because the latter requires that

the density of the Proterozoic sediments be at least 2.84 x 10^3kg m^{-3}, a value which cannot easily be substantiated. A third alternative model, that with a vertical fault, was discounted because it did not satisfy the observed data set as well as did either of the above models, and furthermore, it also required the high Proterozoic density of 2.84 x 10^3kg m^{-3}.

INTRODUCTION

The Norman Range is part of the northern Franklin Mountains which lie on the outer limit of the Mackenzie fold belt (Figure 1). Geological studies of the northern Franklin Mountains by Cook and Aitken (1973) showed that individual ranges within this mountain belt were formed either by thrust plates or by anticlines aligned along dominant structural trends. A geologic sketch map of the area, compiled by Cook and Aitken (1973) is shown in Figure 2. They concluded that most of the northern Franklin Mountains are probably underlain by a decollement zone within evaporite beds of the Cambrian Saline River Formation and that tectonic thickening of this formation occurred during thrusting and horizontal shortening of the sedimentary cover.

However, after further studies, Cook and Aitken (1976) made an alternative proposal that the observed structures in the Norman Range are also consistent with high-angle reverse faulting involving sub-Saline River strata. This interpretation is also suggested by the fact that Protozeroic sediments are definitely involved in the deformation in the McConnell Range to the southeast (Cook and Aitken; 1973, 1976). Davis and Willott (1978) documented a convincing case for deeper-than-Saline-River

Figure 1:

Generalised location map. The gravity profile starts at Norman Wells.

(after Cook and Aitken, 1973)

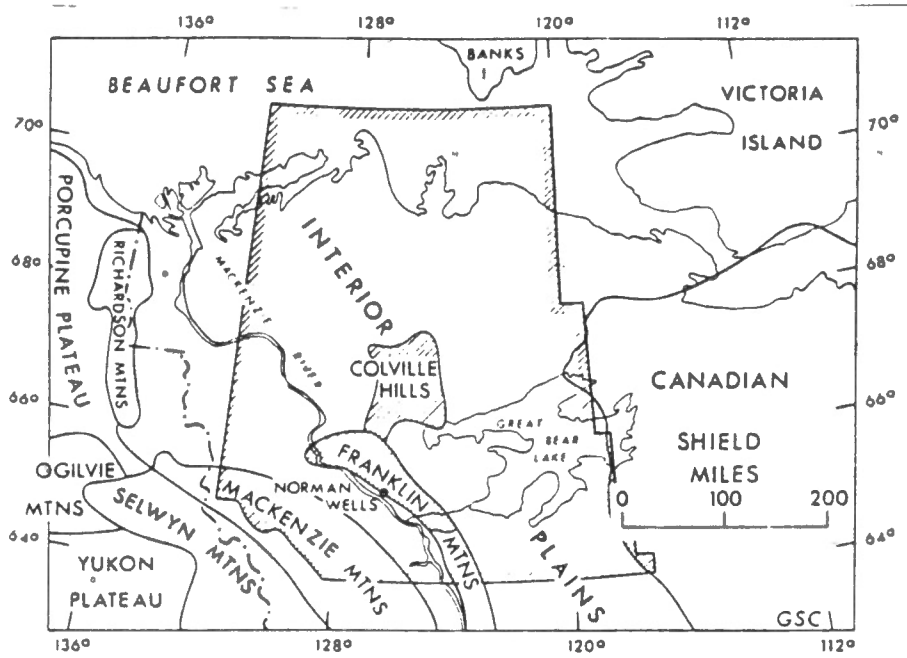

Figure 2:

Geological sketch map of the northern Franklin Mountains.

The area of Figure 3 is indicated.

Note: The Ronning Group is named the Franklin Mountain Formation in this study.

(after Cook and Aitken, 1973)

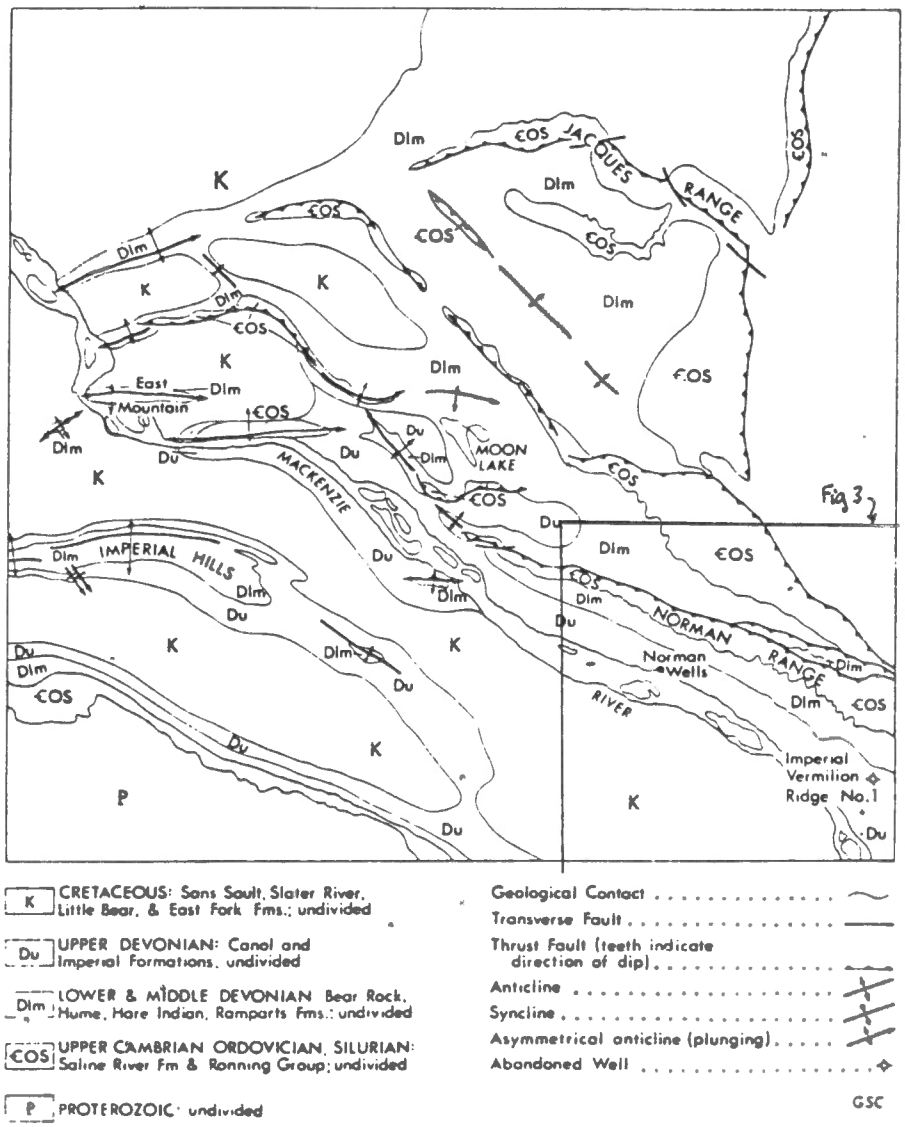

Table 1: Geology and physical properties of formations exposed in the Norman Range

	Formation	Lithology*	Thickness+ range (m)	Well log Density x 10^3 kg m^{-3}	Measured Density x 10^3 kg m^{-3}	Modelling Density x 10^3 kg m^{-3}
DEVONIAN UPPER	IMPERIAL	shale; sandstone; minor limestone	0 to 300	2·50 ± 0·20	-	2·45
	CANOL	black shale, siliceous, bituminous	30 to 100	2·25 ± 0·02	2·23 ± 0·01	2·25
	RAMPARTS	skeletal-fragmental limestone; local shale	30 to 50	2·65 ± 0·03	2·63 ± 0·03	2·64
MID	HARE INDIAN	shale; minor siltstone and limestone	150	2·45 ± 0·20	-	2·45
	HUME	limestone, fossiliferous; minor shale	100	2·70 ± 0·04	2·70 ± 0·01	2·70
LOWER	BEAR ROCK	anhydrite; dolomite; gypsum; solution breccia	230	2·90 ± 0·02	2·70 ± 0·05	2·90
	FRANKLIN MOUNTAIN	dolomite, undifferentiated	500	2·82 ± 0·05	2·83 ± 0·05	2·84
CAMBRIAN	SALINE RIVER	shale; siltstone; salt, undifferentiated	400	-	-	2·30 (assumed)

*Descriptions from Cook and Aitken (1975)

+These data are thickness used for initial models. The thicknesses shown on Figures 4 and 5 are after computer modelling.

deformation in the Coleville Hills. They interpreted that the deep deformation involves basement faults, and extrapolated their Coleville Hills model to include the geometrically similar Franklin Mountains.

In an attempt to resolve the depth to the decollement zone, the Geological Survey of Canada contracted with the writer to undertake a gravity survey with the specific objective of determining whether or not the Saline River Formation has been tectonically thickened within the core of the Norman Range. The general geology of the Paleozoic rocks which are exposed in the study area is summarised in Table 1. Because salt has a significantly lower density than the dolomites, limestones and shales which make up the majority of the sedimentary sequence, it was anticipated that thickening of the Saline River Formation would be manifested by a relative negative gravity anomaly which could be observed at the ground surface.

The Norman Range was selected for the study because it can be approximated to be a two-dimensional structure, and subsurface control is available from well data associated with the Norman Wells oilfield.

DATA ACQUISITION

Fieldwork was conducted in July, 1980. One hundred and eighteen gravity stations were established along a profile of 16 km length. The profile begins on the eastern bank of the Mackenzie River, at the southern end of the Norman Wells oilfield, and terminates to the northeast about 1 km past Oscar Creek (see Figure 3). The average station spacing was 200 m, but this reduced to 50 m in areas of irregular topography on the lower southern slopes of the Norman Range. Access was by vehicle as far

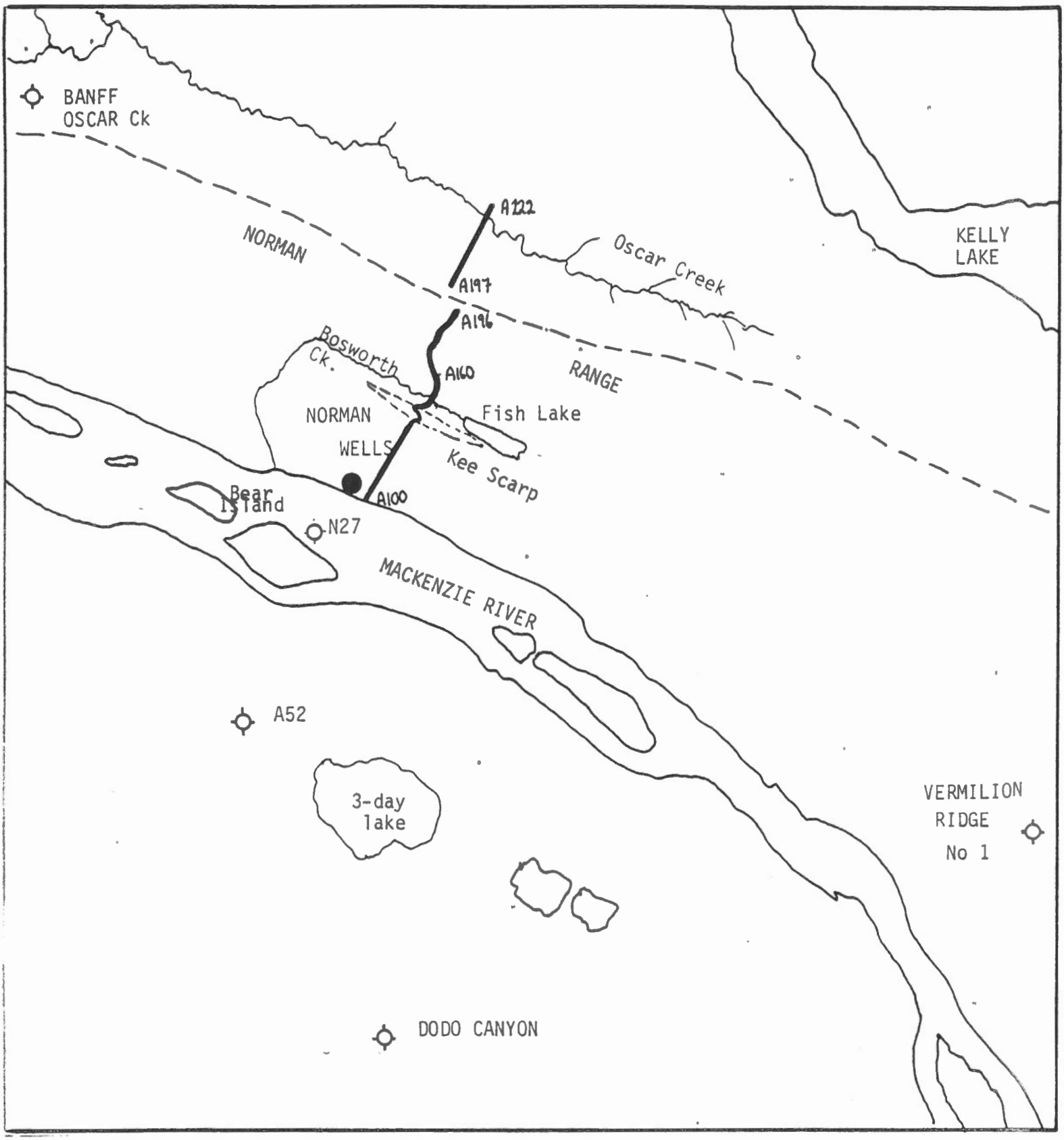

Fig 3. Gravity Profile and well control points.

Scale 1:250,000

Wells

Gravity profile

N

as Kee Scarp (Figure 3) and then by foot or helicopter over the remainder of the profile. A cut line was established between Bosworth Creek and the open tops of the main range.

Wherever possible, the line was kept perpendicular to the main strike direction of the Norman Range (about 110^{o}), but local deviations were necessary to avoid unfavourable topography. During later analysis, the data were projected onto a straight line with an azimuth of 022^{o}.

Stations between A100 and A196, and between A197 and A222 inclusive were surveyed for position and elevation with Wild RDS self-reducing tacheometer and stadia. The southern end of the profile was tied in to an Earth Physics Branch gravity station at the Norman Wells airport terminal, but no closure could be obtained because of the single profile. However, independent fore and back sights were made to each station and the resultant station error is estimated to be ± 5 cm in elevation and ± 2 m in position. The elevation difference between stations A196 and A197 was determined by repeated measurements with a Paulin barometric altimeter, during which time a recording barograph was maintained to monitor atmospheric pressure changes. Temperature corrections were applied and the relative elevation is considered to be accurate to within ± 3 m. The relative position of station A197 with respect to station A196 was determined from aerial photographs.

Gravity measurements were made with a Worden Master gravity meter. Base stations were established along the profile and reoccupied every 1½ to 2 hours to record instrument and diurnal drift. These base stations were later tied in to the airport base station by helicopter traverses. Approximately 10% of the stations were independently reoccupied to check for

reproducibility which was found to be within ± 1 μms^{-2} (1 gravity unit) after drift corrections had been applied.

DATA REDUCTION

The raw gravity data were corrected for drift and relative latitude, and the elevation, Bouguer plate and topographic reductions calculated assuming a reference density of 2.67 x 10^3 $kg \cdot m^{-3}$. The Bouguer anomalies and station data are given in Appendix 1. Topographic corrections were calculated out to Hammer zone M (21.95 km).

The value of the regional gravity field was defined by correcting the observed Bouguer anomaly at station A100 for the gravitational effect of the Paleozoic sediments, assuming that each unit could be considered an horizontal plate of infinite extent. Control of the thickness and density of each formation was available from various wells which are shown in Figure 3. As a result of later gravity modelling a small southwest to northeast regional gradient of + 1 μms^{-2} km^{-1} was also removed; this gradient is due to the gentle westward dip of the basement.

DATA INTERPRETATION

The calculated regional field was subtracted from the observed Bouguer anomalies to yield residual Bouguer anomalies which reflect the density structure within the Norman Range; these residual anomalies are plotted in the upper parts of Figures 4 and 5. The graphs show that there is a relative maximum of + 70 μms^{-2} near station A160 on the southern flank of the range (see Figure 3). Tectonic thickening of the Saline River Formation is negated because there is no evidence of a relative negative

anomaly over the main part of the range. High frequency scatter of the data points, particularly towards the summit of the Norman Range, is caused by local topographic effects and near-surface density variations. The negative anomaly at the southern end of the profile is caused by an increasing thickness of lower density shale sequences.

Control for the interpretation of the data was provided by:

(a) Outcrop geology. Good control of outcrop width and average dips (13^{o} to 15^{o} SW) of sediments exposed along the gravity profile was obtained from Geological maps compiled by Cook and Aitken (1976). Some extrapolation of formation boundaries was necessary in Oscar valley, where there are few exposures.

(b) Well data. Stratigraphic thicknesses and average densities of the formations were obtained from wells associated with the Norman Wells oilfield and exploratory wells in the general area. These data are included in Table 1.

(c) Density measurements. Hand specimens of all the units except the Imperial Formation, Hare Indian Formation, Saline River Formation, and the Proterozoic sediments were collected during the field studies. The dry and wet densities of three independent samples of each lithology were measured and these data are also included in Table 1. Generally the measured values agree closely with the average densities determined from density logs except for the Bear Rock Formation, in which the measured values are significantly lower. This is due to the near-surface dissolution of the anhydrite into dolomite solution breccia of lower density. The densities which are used for the computer models are shown in the last

column of Table 1. A density of 2.30×10^3 kg m^{-3} was assumed for the Saline River Formation since no control was available; this value is a realistic average value for an evaporite and shale sequence.

In addition to the above controls, various assumptions were also made to provide constraints on the density structure in the subsurface. These assumptions were:

(a) that the stratigraphic thicknesses were constant along the section unless otherwise altered by the results of gravity modelling.

(b) that the formation densities were constant along the section.

(c) that the major structures were two-dimensional.

Since the gravity method suffers from the inverse potential problem; i.e. any gravity anomaly has a large number of possible solutions, the assumptions made are justified because the models then represent the least complex structure.

Density models along the section were constructed from the known boundary conditions and the various assumptions, and the theoretical residual gravity anomaly at each station was evaluated by a two-dimensional gravity modelling computer program written and described by Lawton (1979). The calculated anomalies were compared with those observed and the models refined until a good fit was obtained between the data sets. In view of the noise evident in the observed data, a fit to within $\pm$ 5 μms^{-2} was considered satisfactory. The results of the analysis lead to there being three possible alternative solutions to the subsurface density structure.

These final models are shown in the lower parts of Figures 4, 5, and 6 and the calculated anomalies are plotted above the section in each case. The equivalent numerical data are given in Appendices 2, 3, and 4 respectively. However, the first model (Figure 4) is considered most likely to represent the structure of the Norman Range.

Saline River detachment model (Figure 4). In this model, the observed relative positive gravity anomaly is interpreted to be caused by repetition of dense dolomites and anhydrites of the Franklin Mountain, Hume and Bear Rock Formations (Table 1). To place this repeat in its correct spatial position relative to the anomaly maximum, a low angle thrust fault is inferred. Detachment is entirely within the Saline River Formation which has become tectonically thickened in the southwestern part of the section (stations A100 to A120) and locally thickened below the summit of the Norman Range (stations A188 to A196). There is no involvement of sub-Saline River sediments in this deformation model. High-angle reverse faults mapped in the summit region by Cook and Aitken (1975) are considered to be minor secondary faults off the main thrust, which requires at least 9 km of shortening of the post Proterozoic sediment cover.

Proterozoic detachment model (Figure 5). In this model, the major structure is inferred to be a high-angle reverse fault with the core of the Norman Range infilled with Protozeroic sediments; i.e. the deformation involves sub-Saline River strata. Secondary en echelon reverse faults cause additional minor offsets in the summit region. Total horizontal shortening is only about 3 km. However, for this model to generate the relative positive gravity anomaly which is observed, the Proterozoic sediments are required to have a density of at least 2.84×10^3 kg m^{-3} (i.e. a dolomite

lithology). Although the gravity data were reduced relative to an assumed density of 2.67 x 10^3 kg m^{-3}, the effect of a higher density in the Lower Cambrian and Precambrian below the decollement zone would be compensated in the removal of the regional field; the residual Bouguer anomalies would remain essentially unchanged.

Vertical fault model (Figure 6). In this model, the Norman Range scarp is interpreted to be caused by a vertical fault which has a throw of 1.5 km. There is no horizontal shortening involved and the structure is entirely caused by block faulting of the Proterozoic and basement rocks. However, as in the Proterozoic detachment model (Figure 5), it is necessary that the Proterozoic sediments have the higher density of 2.84 x 10^3 kg m^{-3} (dolomite lithology). In the critical summit region of the profile (stations A182-A200), the fit between the computed and observed data is poorer than in either of the other two models, and further deteriorates if a more reasonable Proterozoic density of 2.67 x 10^3 kg m^{-3} is used.

In all final models, the Ramparts Formation has to significantly thicken where it outcrops at the Kee Scarp (stations A130 to A142), to enable a good fit between the observed and calculated anomalies to be obtained. This may represent a reef to back-reef facies.

DISCUSSION AND CONCLUSIONS

The Saline River detachment model is preferred to either of the two models indicating Proterozoic involvement because both these models require the high density of 2.84 x 10^3 kg m^{-3} for the Protozeroic sediments. The only evidence to support this high density value is that Proterozoic dolomites occur in the subsurface north of the Franklin Mountains (D. Pugh, personal

communication). To yield the positive anomaly observed, these dolomites would have to be at least 2000 m thick so that density variations deeper in the section would not have any significant effect at the surface. There is no evidence to substantiate this required thickness and density in the Norman Range area.

The vertical fault model is also rejected because of the poor fit between the observed and calculated Bouguer anomalies in the Norman Range summit region. In this area, the calculated data are the most sensitive to the structural model inferred, and a better fit could not be obtained without requiring a geologically unreasonable density structure.

The preference for the Saline River detachment also arises because the final model is consistent with all the initial premises and no unsubstantiated assumptions had to be invoked. Furthermore, tectonic thickening of the Saline River Formation between stations A100 and A120 is also consistent with thickening of this formation in the Vermillion Ridge Well about 35 km to the southeast (Figure 3). The thickening of the salt has a similar disposition to the main structural features in both areas.

Although Cook and Aitken (1976) preferred the Proterozoic detachment model to the Saline River detachment model because of high-angle short displacement reverse faults being observed elsewhere in the northern Franklins, it is considered here that these structures can indeed be accommodated in the Saline River detachment model. Those faults are considered minor, secondary features associated with flexing of the main thrust sheet (Figure 4).

It is unfortunate that the gravity study has not been able to explicitly resolve the question of Proterozoic involvement in the Norman Range

deformation. However, the model of detachment within the Saline River Formation is preferred, and this may be resolved when further data are available with the development of the Norman Wells oilfield. Both detachment models in fact have economic importance. The Saline River detachment model indicates that the Ramparts Formation (main reservoir rock) extends below the Norman Range in the lower thrust sheet, whereas the Proterozoic detachment model favours structural traps in Lower Cambrian sands which are considered to be potential plays.

D.C. Lawton
Assistant Professor
Department of Geology & Geophysics
University of Calgary

ACKNOWLEDGEMENTS

Dr. D. Cook of the Institute of Sedimentary and Petroleum Geology introduced the structure and stratigraphy of the area and provided much useful data and advice during the interpretation procedure. Mr. D. Pugh, also of the ISPG, provided much of the well information and general stratigraphic correlations. Mr. Brent McLean ably assisted in the field studies.

REFERENCES

Cook, D.G. and Aitken, J.D., 1973, Tectonics of the northern Franklin Mountains and Colville Hills, District of Mackenzie, Canada, in Arctic Geology: Am. Assoc. Pet. Geol., Mem. 19, p. 13-22.

Cook, D.G. and Aitken, J.D., 1975, 1:250,000 geological map of the Norman Wells region: Department of Energy, Mines and Resources.

Cook, D.G. and Aitken, J.D., 1976, Two cross-sections across selected Franklin Mountain structures and their implications for hydrocarbon exploration: Geological Survey of Canada, Paper 76-1B.

Davis, J.W. and Willott, R., 1978, Structural geology of the Colville Hills: Bull. of Canadian Pet. Geol., v. 26, no. 1, p. 105-122.

Lawton, D.C., 1979, Geophysical exploration of titanomagnetite sand deposits, west coast, North Island, New Zealand: Unpublished Ph.D. thesis, University of Auckland.

APPENDIX 1

Station survey data, Observed Bouguer anomalies and topographic corrections

Position and elevation coordinates are in metres. Origin is at station A100
Bouguer anomalies and topographic corrections are in milligal (mgal), where
1 mgal = 10 gravity units.

STAT	X (mN)	Y (mE)	ELEVATION (m)	BOUGUER ANOM (mgal)	TOPOGRAPHIC CORRECTION (mgal)
100	0.0	0.0	59.4	193.3	-0.5
101	75.3	25.1	63.9	193.5	-0.5
102	235.3	81.9	66.4	193.6	-0.5
103	386.1	126.7	69.4	193.8	-0.5
104	517.7	171.5	68.1	193.8	-0.5
105	617.2	282.1	66.9	194.0	-0.5
106	714.1	388.5	64.8	194.2	-0.5
107	800.8	490.2	61.6	194.3	-0.6
108	938.6	581.5	62.2	194.4	-0.6
109	1051.7	687.9	65.3	194.8	-0.7
110	1146.2	787.9	71.2	194.8	-0.7
111	1248.9	894.5	75.0	194.7	-0.7
112	1352.9	1003.6	80.0	194.7	-0.7
113	1511.3	1174.1	91.3	194.8	-0.8
114	1615.6	1305.8	94.4	195.0	-0.8
115	1727.1	1402.8	97.2	195.0	-0.8
116	1831.1	1509.3	104.4	195.1	-0.8
117	1927.5	1607.9	111.4	195.2	-0.9
118	2027.1	1708.6	118.4	195.3	-0.9
119	2126.8	1810.1	124.0	195.4	-0.9
120	2234.2	1932.0	129.3	195.5	-0.9
121	2322.9	2027.1	132.6	195.9	-1.0
122	2432.5	2133.3	136.0	196.6	-1.1
123	2526.7	2251.3	142.7	197.1	-1.3
124	2618.7	2388.9	158.8	198.0	-1.7
125	2605.8	2638.5	162.6	198.5	-2.1
126	2578.2	2840.8	171.9	198.5	-1.9
127	2618.2	2936.6	187.9	198.6	-1.8
128	2691.5	2862.8	196.0	198.5	-1.7
129	2834.3	2802.0	212.1	198.6	-1.6
130	2883.9	2764.7	216.8	198.4	-1.4
131	2988.7	2681.1	227.1	198.5	-1.4
132	3049.6	2638.4	232.3	198.6	-1.4
133	3064.2	2785.0	243.1	198.7	-1.4
134	3098.6	2874.1	251.1	198.9	-1.4
135	3133.2	2972.6	257.0	199.2	-1.5
136	3166.9	3109.2	266.4	199.2	-1.4
137	3227.9	3163.9	275.7	199.1	-1.2
138	3336.0	3199.2	283.4	199.3	-1.2
139	3453.3	3250.8	290.9	199.4	-1.2
140	3531.9	3269.9	296.9	199.9	-1.6
141	3681.3	3198.6	320.4	199.8	-1.8
142	3879.0	3318.1	310.9	199.9	-1.5
144	4058.8	3405.1	242.7	200.8	-1.7
145	4186.3	3430.1	241.3	201.1	-1.5
146	4291.4	3510.9	244.5	201.3	-1.3
147	4431.9	3548.9	246.4	201.9	-1.5
148	4571.2	3541.7	247.2	202.0	-1.5
150	4738.9	3500.7	256.8	202.4	-1.9
151	4765.1	3497.4	264.0	202.8	-2.1
152	4845.4	3491.5	265.9	203.3	-2.2
153	4893.4	3485.4	275.6	203.4	-2.2
154	4965.5	3498.1	285.9	203.4	-2.3
155	5018.6	3503.1	305.0	203.6	-2.4
156	5070.2	3509.2	316.8	203.8	-2.5
157	5119.3	3510.8	329.7	203.9	-2.7
158	5160.2	3526.7	346.5	203.7	-2.5

159	5214.1	3545.9	369.7	203.7	-2.6
160	5288.9	3572.1	385.5	203.8	-2.5
161	5423.2	3546.5	376.0	204.4	-2.5
162	5501.4	3530.1	371.6	204.0	-2.0
164	5623.7	3472.9	376.6	203.6	-1.6
165	5696.1	3453.5	376.8	204.0	-1.8
167	5769.7	3429.5	386.7	203.9	-1.9
168	5855.6	3407.1	395.0	203.9	-1.9
169	5931.7	3408.2	399.5	204.0	-1.9
171	6110.0	3414.1	437.6	203.6	-2.0
172	6159.6	3343.2	439.5	203.7	-2.1
173	6175.5	3314.7	441.5	203.7	-2.1
174	6217.5	3266.2	439.2	203.9	-2.3
176	6323.3	3246.0	453.3	203.7	-2.4
177	6502.5	3126.9	490.0	204.4	-2.5
178	6640.9	3031.9	517.6	203.4	-3.3
179	6848.7	3061.9	517.2	204.1	-3.4
180	6918.1	3111.9	533.6	204.5	-3.6
181	7162.3	3151.3	595.9	203.6	-3.9
182	7367.6	3274.6	595.4	204.1	-4.2
184	7610.5	3315.5	706.9	203.7	-6.1
185	7797.0	3315.7	733.8	203.3	-5.8
186	7932.2	3370.2	731.7	203.6	-5.4
187	8090.7	3449.3	728.4	203.1	-4.6
188	8207.0	3534.9	759.8	202.3	-4.9
189	8308.1	3588.8	768.3	202.2	-5.1
190	8431.4	3739.9	770.2	201.7	-4.5
191	8536.9	3894.3	779.5	202.0	-5.2
192	8705.0	3981.5	781.1	202.2	-5.4
193	8845.9	4003.2	793.5	202.2	-6.1
194	9059.4	4012.0	825.3	201.0	-7.1
195	9256.6	4050.9	863.2	200.4	-10.3
196	9307.1	4065.4	863.7	200.3	-11.1
197	10330.1	3329.2	525.3	200.1	-2.8
199	10411.5	3869.5	492.3	200.0	-2.5
200	10589.0	3955.3	454.6	200.2	-2.2
201	10708.8	4012.1	430.3	200.4	-2.0
202	10887.8	4095.9	397.3	200.8	-1.8
203	11068.7	4181.0	378.7	201.0	-1.6
204	11245.2	4265.9	364.1	201.0	-1.4
205	11426.1	4351.9	345.3	201.3	-1.2
206	11608.4	4439.0	332.0	201.4	-1.1
207	11788.4	4522.8	323.4	201.5	-1.0
208	11972.0	4608.5	315.9	201.5	-0.9
209	12152.1	4692.5	310.6	201.4	-0.8
210	12334.6	4778.5	306.8	201.5	-0.8
211	12514.4	4862.1	305.8	201.5	-0.8
212	12697.3	4947.7	302.4	201.7	-0.7
213	12879.7	5034.6	296.8	201.8	-0.7
214	12998.8	5092.3	297.5	201.7	-0.7
215	13175.7	5180.1	272.8	201.9	-0.8
216	13355.9	5264.5	265.5	202.0	-0.9
217	13454.4	5311.0	261.4	202.1	-1.0
218	13597.8	5376.0	256.0	202.2	-1.1
219	13836.7	5490.8	297.7	201.9	-1.2
220	14015.2	5579.6	307.4	202.1	-1.3
221	14194.6	5665.8	328.9	202.1	-1.4
222	14374.1	5751.8	354.2	201.9	-1.5
223	18900.0	8250.0	586.8	195.4	-1.6

APPENDIX 2

Gravity modelling output data, Saline River detachment model.
Scale units are 1 s.u. = 500m

Gravity anomaly values are in milligal, where 1mgal = 10 gravity units

RESULTS OF CALCULATIONS (SUMMARISED)

X (su)	Z (su)	g obs (mgal)	g thr (mgal)	g res (mgal)
-9.28	-0.09	-12.60	-0.65	-11.95
0.65	-0.14	-6.74	-6.16	-0.58
0.00	-0.12	-6.70	-5.93	-0.77
0.16	-0.13	-6.51	-6.00	-0.51
0.50	-0.13	-6.43	-6.18	-0.25
0.81	-0.14	-6.25	-6.14	-0.11
1.09	-0.14	-6.27	-6.10	-0.17
1.36	-0.13	-6.09	-5.76	-0.33
1.61	-0.13	-5.90	-5.63	-0.27
1.85	-0.12	-5.82	-5.17	-0.65
2.17	-0.12	-5.74	-4.99	-0.75
2.46	-0.13	-5.36	-5.14	-0.22
2.71	-0.14	-5.37	-5.30	-0.07
2.98	-0.15	-5.49	-5.44	-0.05
3.26	-0.16	-5.51	-5.55	0.04
3.68	-0.18	-5.44	-5.56	0.12
3.97	-0.19	-5.26	-5.52	0.26
4.25	-0.19	-5.27	-5.09	-0.18
4.52	-0.21	-5.19	-5.31	0.12
4.77	-0.22	-5.11	-5.21	0.10
5.03	-0.24	-5.02	-5.26	0.24
5.29	-0.25	-4.94	-5.10	0.16
5.58	-0.26	-4.86	-4.81	-0.05
5.82	-0.27	-4.48	-4.47	-0.01
6.10	-0.27	-3.79	-3.54	-0.25
6.36	-0.29	-3.31	-3.11	-0.20
6.64	-0.32	-2.43	-2.75	0.32
6.80	-0.33	-1.94	-2.28	0.34
6.90	-0.34	-1.95	-2.08	0.13
7.04	-0.38	-1.85	-2.01	0.16
7.12	-0.39	-1.96	-1.96	0.00
7.34	-0.42	-1.87	-1.85	-0.02
7.41	-0.43	-2.08	-1.81	-0.27
7.54	-0.45	-1.99	-1.74	-0.25
7.62	-0.46	-1.89	-1.70	-0.19
7.76	-0.49	-1.80	-1.63	-0.17
7.89	-0.50	-1.61	-1.56	-0.05
8.03	-0.51	-1.32	-1.49	0.17
8.19	-0.53	-1.33	-1.41	0.08
8.34	-0.55	-1.44	-1.32	-0.12
8.57	-0.57	-1.25	-1.19	-0.06
8.83	-0.58	-1.17	-1.03	-0.14
8.99	-0.59	-0.68	-0.94	0.26
9.21	-0.64	-0.79	-0.82	0.03
9.67	-0.62	-0.72	-0.51	-0.21
10.07	-0.49	0.15	-0.14	0.29
10.32	-0.48	0.43	0.18	0.25
10.58	-0.49	0.62	0.54	0.08
10.87	-0.49	1.20	0.95	0.25
11.12	-0.49	1.28	1.32	-0.04
11.40	-0.52	1.66	1.62	0.04
11.45	-0.53	2.06	1.68	0.38
11.59	-0.53	2.55	1.72	0.83
11.68	-0.55	2.65	1.81	0.84
11.82	-0.57	2.64	1.85	0.79
11.92	-0.61	2.83	2.11	0.72

12.02	-0.63	3.02	2.20	0.82
12.11	-0.66	3.12	2.37	0.75
12.20	-0.69	2.91	2.55	0.36
12.32	-0.74	2.91	2.76	0.15
12.47	-0.77	3.00	2.98	0.02
12.71	-0.75	3.58	3.05	0.53
12.84	-0.74	3.17	3.08	0.09
13.02	-0.75	2.76	2.99	-0.23
13.14	-0.75	3.15	2.78	0.37
13.26	-0.77	3.04	2.87	0.17
13.40	-0.79	3.04	2.86	0.18
13.55	-0.80	3.13	2.73	0.40
13.88	-0.88	2.70	2.83	-0.13
13.92	-0.88	2.80	2.72	0.08
13.93	-0.88	2.80	2.68	0.12
13.97	-0.88	3.00	2.54	0.46
14.15	-0.91	2.79	2.52	0.27
14.40	-0.98	3.47	2.78	0.69
14.58	-1.04	2.46	3.03	-0.57
14.99	-1.03	3.13	2.61	0.52
15.16	-1.07	3.52	2.79	0.73
15.64	-1.19	2.59	2.89	-0.30
16.11	-1.19	3.06	2.41	0.65
16.60	-1.41	2.63	2.73	-0.10
16.94	-1.47	2.21	2.49	-0.28
17.23	-1.46	2.49	2.29	0.20
17.59	-1.46	1.97	1.94	0.03
17.87	-1.52	1.15	1.65	-0.50
18.09	-1.54	1.03	1.39	-0.36
18.43	-1.54	0.51	1.19	-0.68
18.75	-1.56	0.79	1.28	-0.49
19.12	-1.56	0.97	1.06	-0.09
19.40	-1.59	0.95	1.06	-0.11
19.80	-1.65	-0.28	0.25	-0.53
20.20	-1.73	-0.90	-0.45	-0.45
20.30	-1.73	-1.01	-0.51	-0.50
22.03	-1.05	-1.32	-0.94	-0.38
22.21	-0.98	-1.43	-1.28	-0.15
22.60	-0.91	-1.26	-1.38	0.12
22.87	-0.86	-1.08	-1.41	0.33
23.26	-0.79	-0.70	-1.36	0.66
23.66	-0.76	-0.53	-0.86	0.33
24.05	-0.73	-0.55	-0.72	0.17
24.45	-0.69	-0.28	-0.66	0.38
24.85	-0.66	-0.20	-0.63	0.43
25.25	-0.65	-0.13	-0.61	0.48
25.65	-0.63	-0.15	-0.58	0.43
26.05	-0.62	-0.28	-0.54	0.26
26.45	-0.61	-0.21	-0.51	0.30
26.85	-0.61	-0.23	-0.49	0.26
27.25	-0.60	-0.06	-0.48	0.42
27.66	-0.59	0.02	-0.17	0.19
27.92	-0.59	-0.10	0.04	-0.14
28.31	-0.55	0.07	0.38	-0.31
28.71	-0.53	0.15	0.37	-0.22
28.93	-0.52	0.23	0.36	-0.13
29.24	-0.51	0.31	0.34	-0.03
29.77	-0.60	-0.02	0.31	-0.33
30.17	-0.61	0.15	0.31	-0.16
30.57	-0.66	0.13	0.28	-0.15
30.96	-0.71	-0.10	0.22	-0.32
41.22	-1.17	-7.26	-0.52	-6.74

APPENDIX 3

Gravity modelling output data, proterozoic detachment model.

Scale units are 1 s.u. = 500m

Gravity anomaly values are in milligal, where 1 mgal = 10 gravity units.

RESULTS OF CALCULATIONS (SUMMARISED)

X (su)	Z (su)	g obs (mgal)	g thr (mgal)	g res (mgal)
-9.28	-0.09	-12.60	-0.74	-11.86
0.65	-0.14	-6.74	-6.54	-0.20
0.00	-0.12	-6.70	-6.39	-0.31
0.16	-0.13	-6.51	-6.45	-0.06
0.50	-0.13	-6.43	-6.59	0.16
0.81	-0.14	-6.25	-6.50	0.25
1.09	-0.14	-6.27	-6.42	0.15
1.36	-0.13	-6.09	-6.04	-0.05
1.61	-0.13	-5.90	-5.87	-0.03
1.85	-0.12	-5.82	-5.38	-0.44
2.17	-0.12	-5.74	-5.14	-0.60
2.46	-0.13	-5.36	-5.24	-0.12
2.71	-0.14	-5.37	-5.35	-0.02
2.98	-0.15	-5.49	-5.44	-0.05
3.26	-0.16	-5.51	-5.50	-0.01
3.68	-0.18	-5.44	-5.43	-0.01
3.97	-0.19	-5.26	-5.33	0.07
4.25	-0.19	-5.27	-4.85	-0.42
4.52	-0.21	-5.19	-5.03	-0.16
4.77	-0.22	-5.11	-4.89	-0.22
5.03	-0.24	-5.02	-4.91	-0.11
5.29	-0.25	-4.94	-4.71	-0.23
5.58	-0.26	-4.86	-4.40	-0.46
5.82	-0.27	-4.48	-4.03	-0.45
6.10	-0.27	-3.79	-3.09	-0.70
6.36	-0.29	-3.31	-2.64	-0.67
6.64	-0.32	-2.43	-2.29	-0.14
6.80	-0.33	-1.94	-1.81	-0.13
6.90	-0.34	-1.95	-1.61	-0.34
7.04	-0.38	-1.85	-1.56	-0.29
7.12	-0.39	-1.96	-1.51	-0.45
7.34	-0.42	-1.87	-1.40	-0.47
7.41	-0.43	-2.08	-1.37	-0.71
7.54	-0.45	-1.99	-1.31	-0.68
7.62	-0.46	-1.89	-1.27	-0.62
7.76	-0.49	-1.80	-1.21	-0.59
7.89	-0.50	-1.61	-1.15	-0.46
8.03	-0.51	-1.32	-1.08	-0.24
8.19	-0.53	-1.33	-1.01	-0.32
8.34	-0.55	-1.44	-0.93	-0.51
8.57	-0.57	-1.25	-0.81	-0.44
8.83	-0.58	-1.17	-0.68	-0.49
8.99	-0.59	-0.68	-0.59	-0.09
9.21	-0.64	-0.79	-0.50	-0.29
9.67	-0.62	-0.72	-0.21	-0.51
10.07	-0.49	0.15	0.14	0.01
10.32	-0.48	0.43	0.45	-0.02
10.58	-0.49	0.62	0.79	-0.17
10.87	-0.49	1.20	1.18	0.02
11.12	-0.49	1.28	1.54	-0.26
11.40	-0.52	1.66	1.81	-0.15
11.45	-0.53	2.06	1.87	0.19
11.59	-0.53	2.55	1.89	0.66
11.68	-0.55	2.65	1.97	0.68
11.82	-0.57	2.64	2.00	0.64
11.92	-0.61	2.83	2.24	0.59

12.02	-0.63	3.02	2.31	0.71
12.11	-0.66	3.12	2.48	0.64
12.20	-0.69	2.91	2.64	0.27
12.32	-0.74	2.91	2.83	0.08
12.47	-0.77	3.00	3.03	-0.03
12.71	-0.75	3.58	3.06	0.52
12.84	-0.74	3.17	3.07	0.10
13.02	-0.75	2.76	2.95	-0.19
13.14	-0.75	3.15	2.72	0.43
13.26	-0.77	3.04	2.79	0.25
13.40	-0.79	3.04	2.75	0.29
13.55	-0.80	3.13	2.58	0.55
13.88	-0.88	2.70	2.61	0.09
13.92	-0.88	2.80	2.49	0.31
13.93	-0.88	2.80	2.45	0.35
13.97	-0.88	3.00	2.30	0.70
14.15	-0.91	2.79	2.24	0.55
14.40	-0.98	3.47	2.45	1.02
14.58	-1.04	2.46	2.67	-0.21
14.99	-1.03	3.13	2.17	0.96
15.16	-1.07	3.52	2.34	1.18
15.64	-1.19	2.59	2.46	0.13
16.11	-1.19	3.06	2.02	1.04
16.60	-1.41	2.63	2.56	0.07
16.94	-1.47	2.21	2.45	-0.24
17.23	-1.46	2.49	2.36	0.13
17.59	-1.46	1.97	2.16	-0.19
17.87	-1.52	1.15	1.91	-0.76
18.09	-1.54	1.03	1.68	-0.65
18.43	-1.54	0.51	1.45	-0.94
18.75	-1.56	0.79	1.45	-0.66
19.12	-1.56	0.97	1.07	-0.10
19.40	-1.59	0.95	0.89	0.06
19.80	-1.65	-0.28	-0.15	-0.13
20.20	-1.73	-0.90	-0.99	0.09
20.30	-1.73	-1.01	-1.07	0.06
22.03	-1.05	-1.32	-1.58	0.26
22.21	-0.98	-1.43	-2.01	0.58
22.60	-0.91	-1.26	-2.07	0.81
22.87	-0.86	-1.08	-1.87	0.79
23.26	-0.79	-0.70	-0.71	0.01
23.66	-0.76	-0.53	-0.16	-0.37
24.05	-0.73	-0.55	-0.04	-0.51
24.45	-0.69	-0.28	0.01	-0.29
24.85	-0.66	-0.20	0.01	-0.21
25.25	-0.65	-0.13	-0.02	-0.11
25.65	-0.63	-0.15	-0.01	-0.14
26.05	-0.62	-0.28	-0.01	-0.27
26.45	-0.61	-0.21	-0.01	-0.20
26.85	-0.61	-0.23	-0.03	-0.20
27.25	-0.60	-0.06	-0.04	-0.02
27.66	-0.59	0.02	0.24	-0.22
27.92	-0.59	-0.10	0.43	-0.53
28.31	-0.55	0.07	0.75	-0.68
28.71	-0.53	0.15	0.72	-0.57
28.93	-0.52	0.23	0.70	-0.47
29.24	-0.51	0.31	0.66	-0.35
29.77	-0.60	-0.02	0.61	-0.63
30.17	-0.61	0.15	0.59	-0.44
30.57	-0.66	0.13	0.55	-0.42
30.96	-0.71	-0.10	0.47	-0.57
41.22	-1.17	-7.26	-0.42	-6.84

APPENDIX 4

Gravity modelling output data, vertical fault model

Gravity anomaly values are in milligal, where 1 mgal = 10 gravity units.

RESULTS OF CALCULATIONS

STAT	X	Z	G RES	G THR	G ERR
1	325.00	-70.00	-6.74	-7.10	0.36
2	0.	-60.00	-6.70	-7.34	0.64
3	80.00	-65.00	-6.51	-7.63	1.12
4	250.00	-65.00	-6.43	-7.25	0.82
5	405.00	-70.00	-6.25	-6.97	0.72
6	545.00	-70.00	-6.27	-6.74	0.47
7	680.00	-65.00	-6.09	-6.52	0.43
8	805.00	-65.00	-5.90	-6.30	0.40
9	925.00	-60.00	-5.82	-6.00	0.18
10	1085.00	-60.00	-5.74	-5.66	-0.08
11	1230.00	-65.00	-5.36	-5.60	0.24
12	1355.00	-70.00	-5.37	-5.54	0.17
13	1490.00	-75.00	-5.49	-5.53	0.04
14	1630.00	-80.00	-5.51	-5.49	-0.02
15	1840.00	-90.00	-5.44	-5.36	-0.08
16	1985.00	-95.00	-5.26	-5.10	-0.16
17	2125.00	-95.00	-5.27	-4.89	-0.38
18	2260.00	-105.00	-5.19	-4.87	-0.32
19	2385.00	-110.00	-5.11	-4.85	-0.26
20	2515.00	-120.00	-5.02	-4.79	-0.23
21	2645.00	-125.00	-4.94	-4.59	-0.35
22	2790.00	-130.00	-4.96	-4.06	-0.90
23	2910.00	-135.00	-4.48	-3.56	-0.92
24	3050.00	-135.00	-3.79	-2.94	-0.85
25	3180.00	-145.00	-3.31	-2.49	-0.82
26	3320.00	-160.00	-2.43	-1.95	-0.48
27	3400.00	-165.00	-1.94	-1.62	-0.32
28	3450.00	-170.00	-1.95	-1.47	-0.48
29	3520.00	-190.00	-1.85	-1.42	-0.43
30	3560.00	-195.00	-1.96	-1.38	-0.58
31	3670.00	-210.00	-1.87	-1.30	-0.57
32	3705.00	-215.00	-2.08	-1.27	-0.81
33	3770.00	-225.00	-1.99	-1.22	-0.77
34	3810.00	-230.00	-1.89	-1.18	-0.71
35	3880.00	-245.00	-1.80	-1.13	-0.67
36	3945.00	-250.00	-1.61	-1.07	-0.54
37	4015.00	-255.00	-1.32	-1.01	-0.31
38	4095.00	-265.00	-1.33	-0.95	-0.38
39	4170.00	-275.00	-1.44	-0.89	-0.55
40	4285.00	-285.00	-1.25	-0.78	-0.47
41	4415.00	-290.00	-1.17	-0.66	-0.51
42	4495.00	-295.00	-0.68	-0.60	-0.08
43	4605.00	-320.00	-0.79	-0.51	-0.28
44	4835.00	-310.00	-0.72	-0.26	-0.46
45	5035.00	-245.00	0.15	0.06	0.09
46	5160.00	-240.00	0.43	0.35	0.08
47	5290.00	-245.00	0.62	0.67	-0.05
48	5435.00	-245.00	1.20	1.05	0.15
49	5560.00	-245.00	1.28	1.18	0.10
50	5700.00	-260.00	1.66	1.61	0.05
51	5725.00	-265.00	2.06	1.63	0.43
52	5795.00	-265.00	2.55	1.71	0.84
53	5840.00	-275.00	2.65	1.74	0.91
54	5910.00	-285.00	2.64	1.81	0.83
55	5960.00	-305.00	2.33	1.34	0.99
56	6010.00	-315.00	3.02	1.88	1.14
57	6055.00	-330.00	3.12	1.91	1.21

| | | |